Published in final edited form as:
J Neurosci. 2011 March 9; 31(10): 3589–3601. doi:10.1523/JNEUROSCI.4310-10.2011.

Spatiotemporal properties of neuron response suppression in owl monkey primary somatosensory cortex when stimuli are presented to both hands

Jamie L. Reed[1], **Hui-Xin Qi**[1], and **Jon H. Kaas**[1,2]

[1] Department of Psychology, Vanderbilt University, 111 21st Ave. S., 301 Wilson Hall Nashville, TN 37240 USA

[2] Center for Integrative and Cognitive Neuroscience, Vanderbilt Vision Research Center, Vanderbilt University, USA

Abstract

Despite the lack of ipsilateral receptive fields (RFs) for neurons in the hand representation of area 3b of primary somatosensory cortex, interhemispheric interactions have been reported to varying degrees. We investigated spatiotemporal properties of these interactions to determine: response types; timing between stimuli to evoke the strongest bimanual interactions; topographical distribution of effects; and their dependence on similarity of stimulus locations on the two hands. We analyzed response magnitudes and latencies of single neurons and multi-neuron clusters recorded from 100-electrode arrays implanted in one hemisphere of each of two anesthetized owl monkeys. Skin indentations were delivered to the two hands simultaneously and asynchronously at mirror locations (matched sites on each hand) and non-mirror locations. Since multiple neurons were recorded simultaneously, stimuli on the contralateral hand could be within or outside of the classical RFs of any given neuron. For most neurons, stimulation on the ipsilateral hand suppressed responses to stimuli on the contralateral hand. Maximum suppression occurred when the ipsilateral stimulus was presented 100ms before the contralateral stimulus onset ($P < 0.0005$). The longest stimulus onset delay tested (500ms) allowed contralateral responses to recover to control levels ($P = 0.428$). Stimulation on mirror digits did not differ from stimulation on non-mirror locations ($P = 1.000$). These results indicate that interhemispheric interactions are common in area 3b, somewhat topographically diffuse, and maximal when the suppressing ipsilateral stimulus preceded the contralateral stimulus. Our findings point to a neurophysiological basis for "interference" effects found in human psychophysical studies of bimanual stimulation.

Keywords

area 3b; bimanual; interhemispheric; multielectrode; primate; Utah array

INTRODUCTION

While other areas of the body are represented bilaterally even in primary somatosensory cortex area 3b, neuronal recordings from the hand representation consistently report receptive fields for monkey area 3b neurons exclusively localized to the contralateral hand (Pons et al., 1987, review), and anatomically, 3b has few callosal connections to directly

Corresponding author: Jamie L. Reed, Ph.D., Department of Psychology, Vanderbilt University, 111 21st Ave. S., 301 Wilson Hall, Nashville, TN 37240, Phone number: 615-322-6029, Fax number: 615-343-8449, jamie.l.reed@vanderbilt.edu.

mediate hand-hand interactions (Killackey et al., 1983). Bilateral receptive fields have been found in the hand representations of higher-level cortical areas, including areas 1, 2, S2 (for review, Iwamura, 2002), and PV (Krubitzer and Kaas, 1990). While it may seem unlikely that stimuli on the two hands interact to influence responses in area 3b, evidence for such interactions exists. Ipsilateral stimulation may provide subthreshold activity that, when combined with contralateral stimulation, results in bimanual interactions. Bilateral responses have been reported in forelimb (e.g., Ogawa et al., 2000) and hindlimb (Shin et al., 1997; Alenda and Nuñez, 2004) portions of rat S1. Several studies have reported evidence for interhemispheric interactions in anterior parietal cortex during bimanual stimulation in humans (e.g., Schnitzler et al., 1995; Hoechstetter et al., 2001; Braun et al., 2005; Zhu et al., 2007) and nonhuman primates (Burton et al., 1998; Tommerdahl et al., 2006). In area 3b of monkeys, interhemispheric interactions have been described as primarily suppressive, in that simultaneous tactile stimulation of both hands suppresses neural activity in area 3b measured on one side through optical imaging (Tommerdahl et al., 2006). Loss of input, through amputation or local anesthesia of an ipsilateral digit for instance, leads to a release from inhibition in contralateral area 3b neurons (e.g., Calford and Tweedale, 1990a,b). Interhemispheric effects likely involve intrahemispheric feedback projections to area 3b from other cortical areas containing neurons with bilateral receptive fields (Calford, 2002, review). The topography of sites producing these suppressive effects has not been well-established, but the effects are expected to be rather widespread based on the diffuse nature of feedback projections (e.g., Cusick et al., 1989; Darian-Smith et al., 1993; Burton and Fabri, 1995; Burton et al., 1995).

We were interested in the effect on responses in 3b when tactile stimuli are presented to the hands asynchronously. Temporal and spatial characteristics of interhemispheric effects may be important in area 3b, but have not been studied systematically. In this study, we presented 500ms skin indentations simultaneously on matching and non-matching locations on the two hands of owl monkeys. For the selected paired locations, we also presented the contralateral stimulus at various onset delays. Thus, we were able to characterize the spatiotemporal stimulation effects on interhemispheric interactions. The results indicate that the responses of many neurons in the hand representation in area 3b of monkeys that are activated by tactile stimuli on the contralateral hand are suppressed by stimulation on the ipsilateral hand. These results suggest a neurophysiological basis for the perceptual effects of bimanual stimulation in humans, in which suprathreshold stimulation on the ipsilateral hand interferes with the ability to perceive a near-threshold tactile stimulus on the contralateral hand (e.g., Braun et al., 2005).

MATERIALS AND METHODS

Preparation

All procedures followed the guidelines established by the National Institutes of Health and the Animal Care and Use Committee at Vanderbilt University. Two adult owl monkeys A and B (*Aotus nancymaae*) were prepared for electrophysiological recordings in the left hemisphere of primary somatosensory cortex following procedures presented in detail previously (Reed et al., 2008, 2010). (Note: these are the same individuals as monkeys 2 and 3, respectively, from Reed et al., 2010.) Monkeys (monkey A, male, 1 kg and monkey B, female, 1.2 kg) were anesthetized with propofol during surgery (10 mg/kg/hr, intravenous) and electrophysiological recording (0.3 mg/kg/hr). During surgery and recording sessions monkeys were paralyzed via vecuronium bromide (0.1–0.3 mg/kg/hr, intravenous) mixed with 5% dextrose and Lactated Ringer's solution and were artificially ventilated with a mixture of N_2O: O_2: CO_2 (75: 23.5: 1.5) at a rate sufficient to maintain peak end tidal CO_2 at ~ 4%. In monkey B, 1.2 mg/kg sufentanil was added to the Lactated Ringer's solution during the surgical procedures in order to stabilize anesthetic depth. Following delivery of

this amount of sufentanil, the monkey was maintained under anesthesia without supplemental sufentanil for the remainder of the experiment. Anesthesia and paralysis ensured that the hand remained stable during stimulation. The animal was carefully monitored to maintain a steady state of anesthesia, specifically monitoring electrocardiograms, breathing, temperature, and electroencephalograms.

As described previously (Reed et al., 2008, 2010), the 100-electrode array (now Blackrock Microsystems, Salt Lake City, UT) with 1mm long electrodes was inserted to a depth of 600μm using a pneumatic inserter so that the electrode tips were expected to be located within layer 3 of cortex. While there is some variability due to the slight curvature of the brain, histological analysis was used to estimate the electrode depth (see Histology).

Tactile Stimulation and Recording Procedures

Our equipment and stimulus parameters have been described previously (Reed et al., 2008, 2010), and were used in these experiments to test responses to paired stimuli applied bimanually to mirror and non-mirror digits. Briefly, stimuli were provided by two independent force- and position-feedback controlled motor systems (300B, Aurora Scientific Inc., Aurora, ON, CA), with contact made by round Teflon probes 1 mm in diameter. Stimuli consisted of pulses that indented the skin 0.5mm for 0.5s, followed by 2.0s off of the skin, repeated for 255s (100 trials). Stimuli were delivered to paired skin sites simultaneously (0ms) or at selected stimulus onset delays of 10, 30, 50, 100, and 500ms of one of the two stimuli. Single-site control stimuli were delivered to the ipsilateral (left hand) and contralateral (right hand) sites prior to paired stimulation. Recordings were made from the left hemisphere. The fingernails were glued (cyanoacrylic) to Teflon screws fixed in plasticine to keep the hand stable during stimulus blocks.

In addition to controlled mechanical stimulation, we used light tactile stimulation to map the minimal receptive fields (mRFs; e.g., Merzenich et al., 1983) of selected electrodes. Receptive field mapping aided our reconstruction of the electrode locations as within and outside of area 3b, to complement our subsequent histological identification of area 3b. As we have published previously (Reed et al., 2008), the mRF was defined as the region of skin in which a near-threshold light touch with a probe reliably evoked spikes from the recorded neurons. Typical procedures for mRF mapping of somatic sensory responses in primates have been published (e.g., Merzenich et al., 1978; Nelson et al., 1980; Jain, Qi, and Kaas, 2001).

Recordings were made using the 100-electrode array and the Bionics Data Acquisition System (now Blackrock Microsystems). The signals on each channel were amplified by 5000 and band-pass filtered between 250 Hz and 7.5 kHz. The response threshold for neurons at each electrode was automatically set for 3.25 times the mean activity and the waveforms were sampled at 30 kHz for 1.5ms windows (Samonds et al., 2003).

Histology

At the end of the experiment the electrode array was removed, animals were perfused with 0.9% saline (pH 7.4) followed by fixative (2% paraformaldehyde in phosphate buffer followed by 2% paraformaldehyde with 10% sucrose in phosphate buffer), and the brains were placed in 30% sucrose solution overnight in preparation for histological analysis. The cortex was flattened between glass slides, frozen, and cut parallel to the surface in 40μm sections. Sections were processed for myelin using the silver staining procedure of Gallyas (1979) with slight modifications (Jain et al., 1998, Jain et al., 2001) to aid in determining the electrode locations relative to the borders of area 3b hand representation (see Supporting Figure 1 of Reed et al., 2008 for example of tissue quality and further description of

estimation of electrode locations). In these sections, the location of an electrode penetration was apparent as a small hole in the tissue. Electrode depth was estimated by identifying the appearance and disappearance of electrode tracks across serial sections through the depth of cortex. Electrodes are no deeper than the last holes and the identification of layers was approximated based on depth estimates and differences in myelin staining across depths, as described by Jain et al. (1998, 2001). The total electrode length is 1mm, therefore, the recordings cannot come from layer 5, which is at a depth of approximately 1.5mm in owl monkeys. The inserter injected the electrodes 0.6mm; thus, recordings predominantly come from layer 3. Single units are unlikely isolated from layer 4 due to the small granular cells and neuron packing density; however, it is possible that some multi-units were recorded from layer 4 from some of the electrodes in monkey B based on our depth estimates.

Data Analysis

SPIKE SORTING—The details of our spike sorting procedures have been described previously (Reed et al., 2008). Briefly, spike waveforms were sorted into single- and multi-units offline with an automatic spike classification program based on the t-distribution Expectation Maximization Algorithm (Shoham et al., 2003) which is part of the Bionics Data Acquisition System. A second spike sorter program, Plexon Offline Sorter (Plexon Inc., Dallas, TX), was used to verify the quality of unit isolation such that single units had refractory periods ≥ 1.2ms; P values ≤ 0.05 for multivariate ANOVA related to cluster separation; and distinct waveform amplitudes and shapes when compared with other activity on the same electrode (Nicolelis et al., 2003). Single- and multi-units were categorized separately but were both included in the same statistical model for factor analysis. When careful analysis of the waveform data showed that not all spikes had similar shapes, amplitudes, and durations, we did not assume that those spikes all came from a single neuron. Thus, waveforms that could not be isolated as from a single unit were termed ‘multi-unit’ recordings. Typically, we obtained multi-unit recordings along with one or more single units, but occasionally the automatic spike sorting program designated units based on waveform shape and amplitude as different unit clusters, even when those units could not be isolated into single units. Multiple single units collected from individual electrodes were included in the analysis; however, when multiple clusters of neuronal waveforms could not be isolated into single units, only one neuron cluster was selected for analysis per electrode. The neuron cluster selected for analysis was chosen by having the highest firing rate.

PEAK FIRING RATE—As described in Reed et al. (2008), to determine peak firing rate, spike trains were smoothed with a spike density function using Matlab (The Mathworks, Inc., Natick, MA). A spike density function was produced by convolving the spike train from each trial with a function resembling a postsynaptic potential specified by τ_g, the time constant for the growth phase, and τ_d, the time constant for the decay phase as:

$$R(t)=(1-\exp(-t/\tau_g)*\exp(-t/\tau_d).$$

Based on physiological data from excitatory synapses, τ_g was set to 1ms (e.g., Mason et al., 1991; Moore and Nelson, 1998). We set τ_d to 5ms (Mason et al., 1991; Moore and Nelson, 1998; Veredas et al., 2005) rather than the common value of 20ms because the transient nature of the on and off responses in primary somatosensory neurons was excessively smoothed at larger values, particularly when stimuli were presented at stimulus onset asynchronies of 10 and 30ms. We examined onset responses within a 50ms response time window from the onset of the stimulus of interest. When stimuli were presented with onset asynchronies, the post-stimulus window began from the onset of the second (contralateral) stimulus; thus, the first (ipsilateral) stimulus acted as a “conditioning stimulus” similar to many other studies (e.g., Gardner and Costanzo, 1980b; Chowdhury and Rasumusson, 2003; Greek et al., 2003).

The excitatory peak firing rate was determined as the maximum of the spike density function within the response time window (50ms), and the average baseline firing rate (calculated over a 500ms window prior to stimulation onset) was subtracted from this value. This peak firing rate value was required to be greater than a threshold value, which was the average baseline firing rate plus two standard deviations of this baseline with a minimum value of 5 spikes/s, as described previously (Reed et al., 2010). When the response did not reach threshold in the response window, responses were examined for significant reductions in firing rate. However, we did not encounter neurons with firing rates suppressed below levels of spontaneous activity in response to contralateral stimulation alone in this sample. Additionally, we did not analyze responses beyond the 50ms response time window, including any responses that may occur after the 500ms stimulus came off of the skin.

RESPONSE LATENCY—Response latencies were calculated using Matlab and determined from spike density function histograms as the initial time when the rate meets the half-height over the threshold value of the peak firing rate within the response time window (see *PEAK FIRING RATE*), as we have previously described (Reed et al., 2010). Results were checked manually for proper assignments. This method of determining excitatory response latency is similar to measures that determine the width or duration of peaks in histograms (e.g., Tutunculer et al., 2006; Davidson et al., 2007) and resembles other calculations of minimal latency. Calculating minimal response latency is useful to determine the initial time in which the neuron's firing rate differs from spontaneous activity for the arrival time of signals, rather than determining the timing of the peak firing rate. We examined peak latency for a subset of the data and found that this resulted in later latency values, but the timing of the peak response only changes by a few milliseconds under differing stimulus conditions.

FIRING RATE MODULATION INDEX—We developed a modulation index based on methods used to describe multisensory integration (Stanford et al., 2005; Alvarado et al., 2007). The observed average firing rate response within the 50ms response window during a given bimanual stimulation condition was compared with the distribution of expected average responses based on summation of the unit's response to the two stimuli presented individually. We described this method in Reed et al. (2010). The modulation categories were "superadditive", "subadditive", "additive", "suppressive", or "no difference" from the response to the contralateral stimulus, similar to the methods of Stanford et al. (2005). "Superadditive" responses were greater than the predicted distribution by 2 times the standard deviation of the distribution, and "subadditive" responses were less than the predicted distribution by 2 times the standard deviation of the distribution.

As an additional quantifier, a percent modulation calculation was also performed similar to the multisensory integration index (Meredith and Stein, 1983; Alvarado et al., 2007) and suppression index (Jiang and Stein, 2003) using the following equations:

$$\%\ \text{modulation} = (\text{FR}_{\text{bimanual stimuli}} - \text{FR}_{\text{contralateral control}})/\text{FR}_{\text{contralateral control}} * 100.$$

These calculations incorporated a correction to subtract the average baseline firing rate from the observed average firing rate, and the overall calculation is a subtraction of the response to the contralateral stimulus from the response to the 2-site stimulation, with the result divided by the response to the contralateral stimulus and multiplied by 100.

RESPONSE FIELD—Since we recorded from multiple neurons simultaneously from 100 electrodes over a 4 × 4 mm area, the stimulus locations were not in the receptive field of neurons at every recording site. We defined excitatory "Response Fields" as those skin

locations where the firing rate for a given neuron was clearly above spontaneous activity (Reed et al., 2010). When a site on the hand was stimulated, that site was classified as *inside* an unit's excitatory Response Field if the peak firing rate after subtracting the average baseline firing rate was greater than or equal to 3 times the standard deviation of the average firing rate for the population of neurons. Typically, responsive single neurons were found in 65 out of 100 recording sites. For a given neuron, responses were compared for all of the locations and all of the stimulus onset intervals that were tested in a given experiment. As more than one stimulation location could be within the Response Field, the location with the greatest firing rate was designated as the *center* of that unit's Response Field. The purpose of designating a *center* was to reflect the characteristics of the receptive fields, which typically have a "hot spot". When the unit firing rate did not meet the criteria to be categorized as *inside*, the location was considered *outside* of the Response Field. Thus, the Response Field is a firing-rate-based estimate similar to the concept of a receptive field (as measured by suprathreshold stimulation) and was used to examine and classify spatial integration. When both hands were stimulated, the Response Field designations during stimulation of the two single sites were combined (see Data Classification).

DATA CLASSIFICATION—Data were classified based on several conditions that were used in a statistical model to estimate the contributions of those factors to the observed latencies and firing rates. These factors were the temporal relationship of the stimuli, the spatial relationship of the stimuli, the neuron's Response Field relationship to the stimuli, and the neuron isolation quality (Figure 1).

For analysis of the bimanual stimulation condition the peak firing rates in response to contralateral and ipsilateral stimulation alone were compared. The condition with the highest firing rate was used for the statistical analysis of the stimulus pairing. This was always the contralateral (right hand) location and never the ipsilateral (left hand location). To assess the effect of the temporal relationship of stimuli, we compared the responses to the contralateral control with the responses of neurons under the paired stimulus conditions including presentations of the ipsilateral stimulus with the contralateral stimulus simultaneously (0ms) or preceding the contralateral stimulus by 10, 30, 50, 100, or 500ms (Figure 1A). The spatial relationship of the stimuli refers to placement of two stimulus probes on mirror or non-mirror locations on the two hands or to the location of a single stimulus probe on one hand (Figure 1B). The relationship of the paired stimuli to the Response Field of a given neuron was included as a factor that could influence the firing rate and latency (Figure 1C). Although we allowed for the possibility that units would respond to the ipsilateral stimulus, the ipsilateral stimulus was outside of the Response Fields of all the units collected and included in this analysis. As such, the combined categories were *outside-outside* (OUT_OUT), *inside-outside* (IN_OUT), and *center-outside* (CN_OUT). Finally, we classified the data into single units (SU) and multi-units (MU) (Figure 1D). We tested all of these categories to determine their influence on response latency and peak firing rate.

Statistical modeling of data: The values we obtained for excitatory response latency and peak firing rate from Matlab were summarized in Excel and imported into SPSS 17.0 (SPSS, Inc., Chicago, IL) for further analysis. The data distributions differed from the normal and Poisson distributions (Kolmogorov-Smirnov 1-sample test); therefore, we employed Generalized Estimating Equations (for correlations in data due to repeated measures) in SPSS to analyze this complex dataset. (For detailed information regarding Generalized Estimating Equations analysis, refer to Liang and Zeger, 1986; Zeger and Liang, 1986; Hardin and Hilbe, 2003.) When the data do not fit the normal distribution, the generalized linear model (including Generalized Estimating Equations) extends linear model theory to accommodate measures drawn from non-normal distributions (Gill, 2001, p. 2) to select a variety of distributions from the exponential family of distributions (Hardin & Hilbe, 2003,

p. 7–8). Refer to Reed and Kaas (2010) for specific details of how we used Generalized Estimating Equations analysis. We tested several parameters, and the final statistical model parameters for both latency and firing rate results were based on a gamma probability distribution with the log link function, a first-order autoregressive correlation matrix, and a robust model estimator. In these models, latency or peak firing rate acted as the dependent variable and the predictor variables included: the temporal stimulus relationship, the spatial relationship of stimuli, the relationship of the stimulus to the Response Field of the neuron unit, and the classification of the unit as a single- or muli-unit. See depictions of the predictor variable categories in Figure 1. The Bonferroni correction for multiple comparisons was applied (in all calculations), and the Wald Chi-Square statistic was used to test the significance of the effects of the statistical model. The Wald Chi-Square test is based on the linearly independent pairwise comparisons among the estimated marginal means. The Generalized Estimating Equations analysis provides estimates of the population averages of the dependent variable based on the values of the predictor variables and provides estimates for the significance of the effects.

RESULTS

We obtained single- and multi-unit recordings from 100-electrode arrays histologically localized to cortical layer 3, primarily from area 3b, of two owl monkeys during stimulation of selected locations on the ipsilateral and contralateral hand. Figure 2 depicts the placement of the electrode arrays in the left hemispheres of each of the monkey cases, as determined from receptive field mapping during the recording procedures and myelin staining patterns in sections of flattened cortex. See Table 1 for a list of the conditions included from each monkey. To select units for analysis we used general inclusion criteria and criteria dependent on the measure (firing rate, latency, or modulation index). Foremost, only neurons from sites judged to be in area 3b were included in this study. Additionally, only one multi-unit was included per electrode. The numbers of units meeting the general criteria for analysis were as follows: 117 single units (SUs) and 152 multi-units (MUs) from case A; and 132 SUs and 121 MUs from case B. Data were collapsed across the two monkeys for a population analysis. The criteria specific to each measure are as follows. For firing rate, we only analyzed responses within 50ms after the stimulus onset; therefore, any responses to the stimulus coming off of the skin were not included. For the latency measure, units had to respond to stimulation to have a latency value. For the modulation index, a control value was needed, so only units that responded to single-site contralateral stimulation could be included in order to determine if dual-site stimulation caused increases, decreases, or no change in firing rate.

A series of example rasters and histograms in Figure 3 shows one neuron’s responses to ipsilateral, contralateral, and bimanual stimulation on matching, mirror locations. We never found responses to ipsilateral stimulation alone, as shown in the example; however, ipsilateral stimulation modulated the response to the onset of contralateral stimulation. (We did not analyze the response when the stimulus was withdrawn from the skin.) Figure 4 shows the responses of the same neuron when the paired stimulation sites were located on non-matching, non-mirror locations. The effects in this example neuron resemble the population results: ipsilateral stimulation suppressed responses to contralateral stimuli, and this effect was slightly more pronounced when the stimuli were presented on mirror locations instead of non-mirror locations, as determined by quantitative analysis reported below.

Variations in peak firing rate and response latency

We collected 1743 SU firing rate observations from 117 SUs and 1911 MU firing rate observations from 152 MUs that met the firing rate inclusion criteria under the

spatiotemporal stimulus conditions. The mean peak firing rate for the data set was 19.37 spikes/s (SD 25.14) and the median peak firing rate was 11.32 spikes/s. We obtained fewer response latencies than firing rate observations because not all firing rates met the response criteria, particularly when neurons were strongly suppressed (i.e., we determined the firing rates even when there was no response peak exceeding 5 spikes/s, and hence, no response latency). We collected 1322 SU response latencies (117 SUs) and 1558 MU response latencies (152 MUs) that met our latency inclusion criteria under the spatiotemporal stimulus conditions. The mean response latency for the dataset over all conditions was 23.74ms (SD 6.91) and the median response latency was 22.20ms.

The modeling analysis predicted that several factors influenced the peak firing rate values; and these spatiotemporal stimulus conditions affected peak firing rate more than latency. Tests of the model effects were performed using the Wald Chi-Square statistic for significance of main effects and selected 2-, 3-, and 4-way interactions (Tables 2, 3). The results for which significance calculations are reported are estimates of the peak firing rate and latency values based on the analysis (rather than observed data values). Deviations between the observed data values and the predicted estimates were slight, and the estimates from the analysis followed the trends in the data. Plots in Figures 5 and 6 are observed values. For the statistical analysis, an individual factor is isolated while the other factors are averaged.

Temporal stimulation relationship—We found decreases in peak response magnitudes compared to contralateral stimulation only (17.44 spikes/s ± 0.59) for all of the temporal stimulation conditions in which the ipsilateral stimulus was presented simultaneously with or preceding the contralateral stimulus. As shown in Figure 5A, maximum suppression was found when the ipsilateral stimulus was presented 100ms before the onset of the contralateral stimulus (for all paired stimulus locations combined) (12.67 spikes/s ± 0.71, $P < 0.0005$). The longest stimulus onset delay of 500ms allowed the contralateral response to decay nearly back to control levels (15.93 spikes/s ± 0.81, $P = 0.428$). The remaining pairwise comparisons with contralateral control stimulation are as follows: 0ms = 14.00 spikes/s ± 0.76, $P < 0.0005$; 10ms = 15.02 spikes/s ± 0.80, $P = 0.003$; 30ms = 14.43 spikes/s ± 0.80, $P < 0.0005$; and 50ms = 14.22 spikes/s ± 0.80, $P < 0.0005$. While not shown on Figure 5, we examined all pairwise comparisons. Notably, stimulation at the 100ms delay was significantly different from all other conditions as follows: contralateral control, $P < 0.0005$; 0ms, $P = 0.042$; 10ms, $P < 0.0005$; 30ms, $P = 0.020$; 50ms, $P = 0.031$; 500ms, $P < 0.0005$. The remaining pairwise comparisons reaching significance were the following conditions compared to the 500ms delay condition: 0ms, $P = 0.004$; 30ms, $P = 0.009$; 50ms, $P < 0.0005$. Thus, the interhemispheric effects on the responses to contralateral stimulation occurred not only when stimuli were presented simultaneously, but they had a maximum suppressive effect when the onset of the ipsilateral stimulus preceded the contralateral stimulus by 100ms. Note, however, that the significance is estimated from the statistical model and differences are small between the comparisons with the 100ms group.

Unlike peak firing rate, the response latency to the contralateral stimulus was not significantly affected by the presentation of the ipsilateral stimulus ($P = 0.094$, Figure 6A). Thus, ipsilateral stimulation in conjunction with contralateral stimulation did not affect the latency of responses, but did affect the peak response magnitude (for all paired stimulus locations combined).

Spatial stimulation relationship—Bimanual stimulation resulted in suppression of peak firing rates compared to contralateral stimulation alone (Contralateral = 17.44 spikes/s ± 0.58; Mirror = 14.62 spikes/s ± 1.03, $P = 0.010$; Non-mirror = 14.08 spikes/s ± 0.80, $P < 0.0005$; Figure 5B). Stimulation on mirror digits was not different from stimulation on non-

mirror digits (P = 1.000). There was no effect of the spatial discordance when we subdivided the conditions to account for non-mirror stimulation on adjacent digits versus nonadjacent digits (P = 0.573, not shown), but note that the sample size for this comparison is small (Table 1). Also, presenting paired stimuli on mirror or non-mirror hand locations did not impact the latency of the response to contralateral stimulation (P = 0.983, Figure 6B). Overall, the interhemispheric effects did not show strong topography.

Response Field relationship—As expected, when both stimuli were outside of the Response Field (OUT_OUT, 6.08 spikes/s ±0.51), the peak firing rates were significantly lower than other conditions when the contralateral stimulus was inside the Response Field (IN_OUT, 25.01 spikes/s ± 2.08; P < 0.0005; CN_OUT, 20.29 spikes/s ± 1.66; P < 0.0005) (Figure 5C). The highest firing rates were found when the contralateral stimulus was within the Response Field of the reference unit, and the responses in these two categories were not significantly different (IN_OUT and CN_OUT, P = 0.229). Thus, the distinction between the center (CN) or "hotspot" and the inside (IN) of the contralateral Response Field was not a source of the variability in the peak firing rates. However, the overall location of the contralateral stimulus in relation to the Response Field of the reference unit had a large effect on the firing rate due to the difference between OUT_OUT compared to IN_OUT and CN_OUT; and the interaction of Response Field with the temporal stimulus relationship was a significant source of the variance in firing rates (P < 0.0005, Table 2).

While the Response Field relationship may exhibit a weak tendency to affect the latency of the response to the contralateral stimulus (P = 0.079, Table 3) such that latencies are longer when the paired stimuli are both outside the Response Field, none of the pairwise comparisons between the Response Field categories were significantly different from each other (Figure 6C). Thus, the Response Field categorization affected the variance in peak firing rates but had little effect on latencies.

Unit isolation—Peak firing rate responses of MUs were slightly but significantly higher than those of SUs (mean MU = 16.05 spikes/s ± 1.06; mean SU = 13.22 spikes/s ± 0.92; P = 0.043; Figure 5D). Similarly, excitatory response latencies of MUs were slightly, but significantly faster than those of SUs (mean MU = 22.37ms ± 0.33; mean SU = 25.44ms ± 0.42; P < 0.0005; Figure 6D).

Statistical interactions—Although the effect of the spatial stimulus relationship was not a significant source of variance in the statistical model, the interaction of temporal stimulus relationship with spatial stimulus relationship was significant for peak firing rate (P = 0.001; Table 2) and for latencies (P = 0.003, Table 3). This interaction effect resulted from the suppression relative to contralateral stimulation (17.44 spikes/s ± 0.59) that was stronger during simultaneous stimulation of mirror locations (13.40 spikes/s ± 1.02; P = 0.002) than simultaneous stimulation on non-mirror locations (14.63 spikes/s ± 1.13, P = 0.328), and the suppression when stimuli were applied asynchronously at 10ms delays was weaker for stimulation on mirror locations (15.99 spikes/s ± 1.16, P = 1.000) than for non-mirror locations (14.11 spikes/s ± 0.42, P = 0.039). In contrast, latencies in response to bimanual stimulation differed most from latencies in response to contralateral stimulation alone (24.76ms ± 0.37) when the stimulation sites were on non-mirror locations and the ipsilateral stimulus preceded the contralateral stimulus by 30ms (22.89ms ± 0.46, P = 0.026). However, this latency difference and all other pairwise differences in latency were very small (1–2ms differences), and were thus not convincing contributions to the variance in latencies.

Notably, the interaction between the temporal stimulation category and the unit isolation was not significant for peak firing rate (P = 0.511, Table 2) or latency (P = 0.863, Table 3). We conclude that single units and multi-units behave similarly rather than differently in

response to the temporal stimulation under our conditions. The 3- and 4-way interactions tested were not significant sources of variance and are not displayed graphically. Since the interaction of all four factors, including the signal isolation, did not contribute to the variance in the peak firing rates (P = 0.114, Table 2) and latencies (P = 0.662, Table 3), our results provided further indications that single- and multi-units appeared to behave in similar ways in response to the spatiotemporal stimulation conditions.

In summary, the peak firing rate in response to contralateral stimulation was affected by the time of onset of the contralateral and ipsilateral stimuli. While there was little difference on average between peak firing rates when the paired stimuli were presented to mirror or non-mirror locations on the hand, there was a significant spatiotemporal interaction (such that stimulation on mirror versus non-mirror locations resulted in firing rate differences depending on the stimulus onset delay). In contrast, the latency in response to the contralateral stimulus was affected little by the spatiotemporal relationship with the ipsilateral stimulus.

Firing Rate Modulation Index

We analyzed the single unit and multi-unit data together for firing rate modulation calculations because single units were not significantly different from multi-units (P = 0.261). Examples to depict population responses from recordings across the 100-electrode array are shown in Figure 7, in which we plotted the peak firing responses in a color map of the array for a subset of stimulus parameters. During stimulation on the contralateral location, groups of neurons were activated with high peak firing rates. Some of these firing rates decreased when a location on the ipsilateral hand was stimulated at the same time as the contralateral hand. When the onset of the ipsilateral stimulus preceded that of the contralateral stimulus, the peak firing rates of the active neurons were often reduced. Individual neuron units (represented by colored squares) sometimes showed different changes in firing rate under the same stimulation parameters, but the color map plots are not easily quantified. Therefore, we calculated a trial-by-trial modulation index for each unit to determine whether paired bimanual stimulation affected the response to the contralateral stimulus at a population level.

When we tallied the response modulation types based on the spatial and temporal stimulus characteristics, we found that stimulation on mirror and non-mirror locations in which the stimulus probes were within or outside of the neuron’s Response Field resulted in the same basic trends (Figure 8A). Thus, stimulating matching sites did not cause stronger modulation than stimulating non-matching sites. Summarizing over the stimulation parameters, we found that the majority of unit responses were suppressed by paired ipsilateral stimulation (1865/2994, 62.3%). About one third (1005/2994, 33.6%) of the unit responses to contralateral stimulation were not significantly changed by ipsilateral stimulation. Only about 4% of unit responses (124/2994) were facilitated by ipsilateral stimulation. The presence of response facilitation is somewhat unexpected, but only a small proportion of responses showed this form of modulation during bimanual stimulation in general.

Facilitation occurred rarely, but when facilitation was found, the ipsilateral stimulus was presented at short onset delays (0, 10, or 30ms) before the contralateral stimulus. The proportions of units showing suppression increased as the stimulus onset delays increased. Particularly when mirror locations were stimulated, the most instances of suppression were found when the ipsilateral stimulus preceded the contralateral stimulus by 100ms. Overall, the dominant effect of a preceding ipsilateral stimulus was to suppress the response to the contralateral stimulus at long onset delays (50, 100, or 500ms).

In addition to the increased number of suppressed responses with increasing stimulus onset delays, the magnitude of the suppression increased as well (Figure 8B). The greatest percentage of suppression occurred when the ipsilateral stimulus preceded the contralateral stimulus by 100ms. The magnitude of facilitation changed in an opposing manner. The magnitude of facilitation was very low when the stimuli were presented at long onset delays, and reached 10% or greater when the stimuli were presented within 10ms of each other. The magnitude of suppression was low, but still around 20% when stimuli were presented at short onset delays, and increased in magnitude when stimuli were presented at long onset delays. In general, both mirror and non-mirror stimulation resulted in the same trends for proportions of units suppressed, facilitated, and unchanged; however, the effects on modulation magnitude were more pronounced when mirror locations were stimulated.

DISCUSSION

Our goal was to determine how primate somatosensory cortex responds to tactile stimuli applied to both hands. We found that ipsilateral stimuli typically reduced responses to stimuli on the contralateral hand (Table 2, Figure 5), with only weak effects on latencies (Table 3, Figure 6). As reported previously (Reed et al., 2010), single neurons had higher mean values for peak firing rates and lower means for latency compared to multi-units. However, as they responded similarly to spatiotemporal stimulation (Tables 2, 3), they are discussed together.

Peak firing rate

Firing was primarily suppressed by bimanual skin indentation compared to contralateral stimulation alone (Figure 5A, B). Maximal suppression occurred when the ipsilateral stimulus preceded the contralateral stimulus onset by 100ms (Figures 5A, 8); however, when adjacent digits on the contralateral hand were stimulated, maximum response suppression in area 3b neurons occurred at interstimulus intervals between 30–50ms (Reed et al., 2010). Thus, maximum response suppression for bimanual stimuli requires larger stimulus onset differences than paired unilateral stimuli. This timing allows for considerable cortical processing steps. However, suppression still existed when both hands were stimulated at shorter onset asynchronies, indicating some processing occurs relatively quickly. Previous studies have not always provided clear evidence for suppressive effects of ipsilateral stimulation on area 3b neurons. For example, Burton et al. (1998) did not find strong effects of pairing ipsilateral with contralateral vibratory stimulation on neurons in area 3b (34 neurons recorded) of macaque monkeys when an ipsilateral stimulus preceded the contralateral stimulus. Human neurophysiological studies have also failed to provide consistent evidence that primary somatosensory cortex is suppressed by bimanual stimulation. For example, in magnetoencephalographic (MEG) studies, Hoechstetter et al. (2001) and Disbrow et al. (2001) found that significant suppressive interactions occurred in secondary somatosensory cortex, but not primary somatosensory cortex. However, evidence for suppressive effects in area 3b was found in other studies. When a digit ipsilateral to the recorded neurons was amputated or anesthetized, the receptive field of the given neuron contralateral to the amputated or anesthetized digit increased in size (Calford and Tweedale 1990, 1991a,b), suggesting the loss of ongoing chronic suppression from the ipsilateral hand. In an optical imaging study in squirrel monkeys, simultaneous stimulation of both hands produced less activity in contralateral areas 3b and 1 than contralateral stimulation alone (Tommerdahl et al., 2006). The fact that we found substantial numbers of neurons unaffected by bimanual stimulation (~ 34% of responses) may relate in part to why suppressive interactions during bimanual stimulation were not always found in primary somatosensory cortex.

As inputs to area 3b are largely excitatory (e.g., Conti and Manzoni, 1994; Gonchar et al., 1995), suppressive effects of ipsilateral hand stimulation are likely mediated locally by activation of inhibitory neurons. Consistent with this possibility, suppression by an ipsilateral stimulus was not universal,(Figure 8A). While facilitative response modulation during bimanual stimulation was not reported by Burton et al. (1998) and Tommerdahl et al. (2006), the proportion of facilitated neurons in our study was low (4%), and was likely revealed by our large sample of simultaneous recordings and our variations in spatiotemporal stimulation. If the facilitative inputs to area 3b that are activated by ipsilateral stimulation contact primarily inhibitory neurons, then such small neurons are less likely to be recorded than larger excitatory pyramidal neurons (e.g., Mountcastle et al., 1969).

In addition, interhemispheric interactions within the area 3b hand representation could occur through other mechanisms. A few callosal connections exist between the hand representations in area 3b of both hemispheres (Killacky et al., 1983), a small portion of which may be inhibitory and cause direct inhibition (Conti and Manzoni et al., 1994) as described in rats (Gonchar et al., 1995). Because bilateral receptive fields and denser callosal connections are found for higher-order somatosensory areas, inhibitory callosal effects on these areas could result in reduced excitatory feedback input to area 3b (Figure 9).

Like Tommerdahl et al. (2006), we did not find significant differences between simultaneous stimulation on mirror and non-mirror hand locations, and only when we stimulated sites asynchronously did we uncover topographic specificity related to interhemispheric interactions (Figures 5B, 8), suggesting that these effects are mediated by diffusely distributed feedback connections from areas 1, 2, S2, and PV (e.g., Cusick et al., 1989; Krubitzer and Kaas, 1990; Darian-Smith et al., 1993; Burton and Fabri, 1995; Burton et al., 1995; Angelucci et al., 2002; Disbrow et al., 2003; Shmuel et al., 2005). However, Tommerdahl et al. (2006) did not find a cortical effect on contralateral hand stimulation with simultaneous ipsilateral foot simulation, indicating that some somatotopic matching is needed for an effect.

Response latency

Response latencies showed very little variation during various types of bimanual stimulation (Figure 6). Although we found a statistical interaction between the temporal stimulus relationship and the spatial stimulus relationship ($P = 0.003$, Table 3), the latency differences were only about 1–2ms.

Effects of bimanual stimulation on latencies of area 3b neurons in primates have not been described. However, with unilateral stimulation of the median nerve of the ipsilateral or contralateral hand alone, the onset latency of the ipsilateral field potential (mean ~ 23ms) in area 3b of macaque monkeys was much longer than the contralateral response (mean ~ 6.4ms), as the ipsilateral response began in extragranular layers rather than granular layers (Lipton et al., 2006). Feedback processes are likely responsible for this ipsilateral cortical activity. The latencies were shorter for local field potentials than for neuron spikes, as they reflect inputs rather than neuron action potentials, and electrical stimulation produces faster activation. Unilateral tactile stimulation activates contralateral and ipsilateral anterior parietal cortex in subsets of human subjects (Zhu et al., 2007) and ipsilateral median nerve stimulation produces evoked potentials (Noachtar et al., 1997; Sutherland and Tang, 2006) in anterior parietal fields. Electrical median nerve stimulation in humans causes unnatural sensations and causes activation in ipsilateral area 3b in primates while tactile stimulation does not (e.g., Lipton et al., 2006 [macaque]; Zhu et al., 2007 [human]). Imaging and evoked potential measures likely include subthreshold neuron activity, unlike our electrophysiological measures of spiking output only.

Considerations and Significance

As our studies were performed in anesthetized animals, the effects reflect responses to passive stimulation without influence of attention or task-relevance. While advantages of using anesthetized animals include hand stability for reproducible stimulation conditions over a large stimulus battery and removal of fluctuations due to attention, neuronal responses under anesthesia are not equivalent to responses in unanesthetized animals. Effects of propofol, the anesthetic in this experiment, are not fully known, but it is believed to act primarily as a $GABA_A$ receptor agonist (e.g., Trapani et al., 2000). With propofol, dose-dependent reductions in the amplitudes of somatosensory evoked potentials and prolonged latencies have been reported in rats (e.g., Logginidou et al., 2003). A predominance of inhibitory effects would be expected under the influence of propofol. However, in awake macaque monkeys, suppression also dominates the results of pairing ipsilateral and contralateral tactile stimulation (Burton et al., 1998).

Our suppression results likely reflect neurophysiological bases of the “interference” effects revealed in psychophysical studies in humans. Braun et al. (2005) found that suprathreshold stimuli applied to the left hand 200 or 500ms before a near-threshold test stimulus on the right hand resulted in the subjects more often incorrectly identifying the location of the test stimulus. Thus, presentation of the ipsilateral stimulus “interfered” with subjects’ ability to correctly localize the contralateral stimulus. Our findings that suprathreshold ipsilateral stimuli suppressed responses to suprathreshold contralateral stimuli in many neurons sampled from area 3b (~ 62% of the responses) correspond well with human psychophysical studies such as Braun et al. (2005).

Our results are consistent with a mechanism through which information from one hemisphere reaches neurons in area 3b of the opposite hemisphere indirectly via callosal connections with higher-order somatosensory areas and feedback connections to area 3b. In a comparative study of primary somatosensory cortex in owl monkeys and macaque monkeys, Killackey et al. (1983) found that the area 3b representations of the hands and feet had sparse callosal connections in owl monkeys, and even sparser callosal connections in macaque monkeys. Thus, direct callosal connections are an unlikely source of the suppression in area 3b, rather, interhemispheric influences are likely to occur via cortical feedback mechanisms. Based on our findings and others’, stimulation on both hands simultaneously results globally in weak suppression in both hemispheres, with facilitation in small populations of neurons. This would permit the most salient stimuli on each hand to activate area 3b neurons in the contralateral cerebral hemisphere, while suppressing responses to minor stimuli. The activity produced by the more salient stimuli would be relayed to higher cortical areas such as area 2 and S2, where neurons with bimanual excitatory receptive fields are found (Iwamura et al., 2002, review). An area 3b suppression of weak stimulus inputs by stronger stimulus inputs also occurs with paired stimuli on two digits of the contralateral hand (Reed et al., 2010). These unimanual and bimanual effects would facilitate tactile discrimination and the sensory guidance of motor responses.

Acknowledgments

We are grateful for guidance, assistance, space, and equipment provided by Dr. AB Bonds throughout these experiments. We thank Drs. M. J. Burish, Z. Zhou, and M. R. Bernard for expert assistance during surgical and recording procedures and Drs. O. Gharbawie and C. Camalier for help collecting data. Matlab scripts were written primarily by Dr. P. Pouget and J. Haitas in collaboration with JLR and J. Cockhren. Dr. F. Ebner provided helpful comments on the manuscript. This work was supported by the James S. McDonnell Foundation (JHK) and NIH grants NS16446 (JHK), F31-NS053231 (JLR).

References

Alenda A, Nuñez A. Sensory-interference in rat primary somatosensory cortical neurons. Eur J Neurosci. 2004; 19:766–770. [PubMed: 14984427]

Alvarado JC, Vaughan JW, Stanford TR, Stein BE. Multisensory versus unisensory integration: contrasting modes in the superior colliculus. J Neurophysiol. 2007; 97:3193–3205. [PubMed: 17329632]

Angelucci, A.; Levitt, JB.; Lund, JS. Anatomical origins of the classical receptive field and modulatory surround field of single neurons in macaque visual cortical area V1. In: Azmita, EC.; DeFelipe, J.; Jones, EG.; Rakic, P.; Ribak, CE., editors. Chapter 29 Progress in Brain Research. Vol. 136. Elsevier Science B.V; 2002. p. 373-388.

Berwick J, Redgrave P, Jones M, Hewson-Stoate N, Martindale J, Johnston D, Mayhew JEW. Integration of neural responses originating from different regions of the cortical somatosensory map. Brain Res. 2004; 1030:284–293. [PubMed: 15571677]

Boloori AR, Stanley GB. The dynamics of spatiotemporal response integration in the somatosensory cortex of the vibrissa system. J Neurosci. 2006; 26:3767–3782. [PubMed: 16597730]

Braun C, Hess H, Burkhardt M, Wühle A, Preissl H. The right hand knows what the left hand is feeling. Exp Brain Res. 2005; 162:366–373. [PubMed: 15827739]

Burton H, Fabri M. Ipsilateral intracortical connections of physiologically defined cutaneous representations in area 3b and 1 of macaque monkeys: projections in the vicinity of the central sulcus. J Comp Neurol. 1995; 355:508–538. [PubMed: 7636029]

Burton H, Fabri M, Alloway K. Cortical areas within the lateral sulcus connected to cutaneous representations in areas 3b and 1: a revised interpretation of the second somatosensory area in macaque monkeys. J Comp Neurol. 1995; 355:539–562. [PubMed: 7636030]

Burton H, Sinclair RJ, Whang K. Vibrotactile stimulus order effects in somatosensory cortical areas of rhesus monkeys. Somatosens Mot Res. 1998; 15:316–324. [PubMed: 9875549]

Calford MB. Dynamic representational plasticity in sensory cortex. Neuroscience. 2002; 111:709–738. [PubMed: 12031401]

Calford MB, Tweedale R. Interhemispheric transfer of plasticity in the cerebral cortex. Science. 1990; 249:805–807. [PubMed: 2389146]

Calford MB, Tweedale R. Acute changes in cutaneous receptive fields in primary somatosensory cortex after digit denervation in adult flying fox. J Neurophysiol. 1991a; 65:178–187. [PubMed: 2016636]

Calford MB, Tweedale R. Immediate expansion of receptive fields of neurons in area 3b of macaque monkeys after digit denervation. Somatosens Mot Res. 1991b; 8:249–260. [PubMed: 1767621]

Chowdhury SA, Rasmusson DD. Corticocortical inhibition of peripheral inputs within primary somatosensory cortex: the role of GABAA and GABAB receptors. J Neurophysiol. 2003; 90:851–856. [PubMed: 12904496]

Conti F, Manzoni T. The neurotransmitters and postsynaptic action of callosally projecting neurons. Behav Brain Res. 1994; 64:37–53. [PubMed: 7840891]

Cusick CG, Wall JT, Felleman DJ, Kaas JH. Somatotopic organization of the lateral sulcus of owl monkeys: area 3b, S-II, and a ventral somatosensory area. J Comp Neurol. 1989; 282:169–190. [PubMed: 2496153]

Darian-Smith C, Darian-Smith I, Burman K, Ratcliffe N. Ipsilateral cortical projections to areas 3a, 3b, and 4 in the macaque monkey. J Comp Neurol. 1993; 335:200–213. [PubMed: 8227514]

Davidson AG, O'Dell R, Chan V, Schieber MH. Comparing effects in spike-triggered averages of rectified EMG across different behaviors. J Neurosci Methods. 2007; 163:283–294. [PubMed: 17477974]

Disbrow E, Roberts T, Poeppel D, Krubitzer L. Evidence for interhermispheric processing of inputs from the hands in human S2 and PV. J Neurophysiol. 2001; 85:2236–2244. [PubMed: 11353038]

Disbrow E, Litinas E, Recanzone GH, Padberg J, Krubitzer L. Cortical connections of the second somatosensory area and the parietal ventral area in macaque monkeys. J Comp Neurol. 2003; 462:382–399. [PubMed: 12811808]

Gallyas F. Silver staining of myelin by means of physical development. Neurol Res. 1979; 1:203–209. [PubMed: 95356]

Gonchar YA, Johnson PB, Weinberg RJ. GABA-immunopositive neurons in rat neocortex with contralateral projections to S-I. Brain Res. 1995; 697:27–34. [PubMed: 8593589]

Greek KA, Chowdhury SA, Rasmusson DD. Interactions between inputs from adjacent digits in somatosensory thalamus and cortex of the raccoon. Exp Brain Res. 2003; 151:364–371. [PubMed: 12802551]

Hardin, JW.; Hilbe, JM. Generalized estimating equations. Boca Raton, FL: Chapman and Hall/CRC; 2003. p. 58-76.

Hoechstetter K, Rupp A, Stančák A, Meinck H-M, Stippich C, Berg P, Scherg M. Interaction of tactile input in the human primary and secondary somatosensory cortex—A magnetoencephalographic study. Neuroimage. 2001; 14:759–767. [PubMed: 11506548]

Iwamura Y, Tanaka M, Iriki A, Taoka M, Toda T. Processing of tactile and kinesthetic signals from bilateral sides of the body in the postcentral gyrus of awake monkeys. Behav Brain Res. 2002; 135:185–190. [PubMed: 12356449]

Jain N, Catania KC, Kaas JH. A histologically visible representation of the fingers and palm in primate area 3b and its immutability following long term deafferentation. Cereb Cortex. 1998; 8:227–236. [PubMed: 9617917]

Jain N, Qi H-X, Catania KC, Kaas JH. Anatomic correlates of the face and oral cavity representations in the somatosensory cortical area 3b of monkeys. J Comp Neurol. 2001; 429:455–568. [PubMed: 11116231]

Jain, N.; Qi, H-X.; Kaas, JH. Long-term chronic multichannel recordings from sensorimotor cortex and thalamus of primates. In: Nicolelis, MAL., editor. Chapter 5 of Progress in Brain Research. Vol. 130. Elsevier Science B.V; 2001. p. 1-10.

Kaas JH. The reorganization of somatosensory and motor cortex after peripheral nerve or spinal cord injury in primates. Prog Brain Res. 2000; 128:173–179. [PubMed: 11105677]

Killackey HP, Gould HJ III, Cusick CG, Pons TP, Kaas JH. The relation of corpus callosum connections to architectonic fields and body surface maps in sensorimotor cortex of new and old world monkeys. J Comp Neurol. 1983; 219:328–419. [PubMed: 6619341]

Krubitzer LA, Kaas JH. The organization and connections of somatosensory cortex in marmosets. J Neurosci. 1990; 10:952–974. [PubMed: 2108231]

Li L, Rema V, Ebner FF. Chronic suppression of activity in barrel field cortex downregulates sensory responses in contralateral barrel field cortex. J Neurophysiol. 2005; 94:3342–3356. [PubMed: 16014795]

Liang K-Y, Zeger SL. Longitudinal data analysis using generalized linear models. Biometrika. 1986; 73:13–22.

Lipton ML, Fu K-MG, Branch CA, Schroeder CE. Ipsilateral hand input to area 3b revealed by converging hemodynamic and electrophysiological analyses in macaque monkeys. J Neurosci. 2006; 26:180–185. [PubMed: 16399685]

Logginidou HG, Li B-H, Li D-P, Lohmann JS, Schuler G, DiVittore NA, Kreiser S, Cronin AJ. Propofol suppresses the cortical somatosensory evoked potential in rats. Anesth Analg. 2003; 97:1784–1788. [PubMed: 14633560]

Marcano-Reik AJ, Blumberg MS. The corpus callosum modulates spindle-burst activity within homotopic regions of somatosensory cortex in newborn rats. Euro J Neurosci. 2008; 28:1457–1466.

Mason A, Nicoll A, Stratford K. Synaptic transmission between individual pyramidal neurons of the rat visual cortex in vitro. J Neurosci. 1991; 11:72–84. [PubMed: 1846012]

Merzenich MM, Kaas JH, Sur M, Lin CS. Double representations of the body surface within cytoarchitectonic areas 3b and 1 in “SI” in the owl monkey (*Aotus trivirgatus*). J Comp Neurol. 1978; 181:41–74. [PubMed: 98537]

Merzenich MM, Kaas JH, Wall J, Nelson RJ, Sur M, Felleman D. Topographic reorganization of somatosensory cortical areas 3b and 1 in adult monkeys following restricted deafferentation. Neuroscience. 1983; 8:33–55. [PubMed: 6835522]

Moore CI, Nelson SB. Spatio-temporal subthreshold receptive fields in the vibrissa representation of rat primary somatosensory cortex. J Neurophysiol. 1998; 80:2882–2892. [PubMed: 9862892]

Mountcastle VB, Talbot WH, Sakata H, Hyvärinen J. Cortical neuronal mechanisms in flutter-vibration studied in unanesthetized monkeys. Neuronal periodicity and frequency discrimination. J Neurophysiol. 1969; 32:452–484. [PubMed: 4977839]

Nelson RJ, Sur M, Felleman DJ, Kaas JH. Representations of the body surface in postcentral parietal cortex of Macaca fascicularis. J Comp Neurol. 1980; 192:611–643. [PubMed: 7419747]

Nicolelis MAL, Dimitrov D, Carmena JM, Crist R, Lehew G, Kralik JD, Wise SP. Chronic, multisite, multielectrode recordings in macaque monkeys. Proc Natl Acad Sci USA. 2003; 100:11041–11046. [PubMed: 12960378]

Noachtar S, Lüders HO, Dinner DS, Klem G. Ipsilateral median somatosensory evoked potentials recorded from human somatosensory cortex. Electroencephalogr Clin Neurophysiol. 1997; 104:189–198. [PubMed: 9186233]

Ogawa S, Lee T-M, Stepnoski R, Chen W, Zhu X-H, Ugurbil K. An approach to probe some neural systems interaction by functional MRI at neural time scale down to milliseconds. Proc Natl Acad Sci USA. 2000; 97:11026–11031. [PubMed: 11005873]

Pons TP, Wall JT, Garraghty PE, Cusick CG, Kaas JH. Consistent features of the representation of the hand in area 3b of macaque monkeys. Somatosens Res. 1987; 4:309–331. [PubMed: 3589287]

Reed JL, Pouget P, Qi H-X, Zhou Z, Bernard MR, Burish MJ, Haitas J, Bonds AB, Kaas JH. Widespread spatial integration in primary somatosensory cortex. Proc Natl Acad Sci USA. 2008; 105:10233–10237. [PubMed: 18632579]

Reed JL, Qi H, Zhou Z, Bernard MR, Burish MJ, Bonds AB, Kaas JH. Response properties of neurons in primary somatosensory cortex of owl monkeys reflect widespread spatiotemporal integration. J Neurophysiol. 2010; 103:2139–2157. [PubMed: 20164400]

Reed JL, Kaas JH. Statistical analysis of large-scale neuronal recording data. Neural Networks. 2010; 23:673–684. [PubMed: 20472395]

Rema V, Ebner FF. Lesions of mature barrel field cortex interfere with sensory processing and plasticity in connected areas of the contralateral hemisphere. J Neurosci. 2003; 23:10378–10387. [PubMed: 14614097]

Samonds JM, Allison JD, Brown HA, Bonds AB. Cooperation between Area 17 neuron pairs enhances fine discrimination of orientation. J Neurosci. 2003; 23:2416–2425. [PubMed: 12657701]

Schnitzler A, Salmelin R, Salenius S, Jousmäki V, Hari R. Tactile information from the human hand reaches the ipsilateral primary somatosensory cortex. Neurosci Lett. 1995; 200:25–28. [PubMed: 8584258]

Shin H-C, Won C-K, Jung S-C, Oh S, Park S, Sohn J-H. Interhemispheric modulation of sensory transmission in the primary somatosensory cortex of rats. Neuroscience Letters. 1997; 230:137–139. [PubMed: 9259483]

Shmuel A, Korman M, Sterkin A, Harel M, Ullman A, Malach R, Grinvald A. Retinotopic axis specificity and selective clustering of feedback projections from V2 to V1 in the owl monkey. J Neurosci. 2005; 25:2117–2131. [PubMed: 15728852]

Shoham S, Fellows MR, Normann RA. Robust, automatic spike sorting using mixtures of multivariate t-distributions. J Neurosci Methods. 2003; 127:111–122. [PubMed: 12906941]

Shuler MG, Krupa DJ, Nicolelis MAL. Bilateral integration of whisker information in the primary somatosensory cortex of rats. J Neurosci. 2001; 21:5251–5261. [PubMed: 11438600]

Stanford TR, Quessy S, Stein BE. Evaluating the operations underlying multisensory integration in the cat superior colliculus. J Neurosci. 2005; 25:6499–6508. [PubMed: 16014711]

Sutherland MT, Tang AC. Reliable detection of bilateral activation in human primary somatosensory cortex by unilateral median nerve stimulation. Neuroimage. 2006; 33:1042–1054. [PubMed: 16997579]

Tommerdahl M, Simons SB, Chiu JS, Favorov O, Whitsel BL. Ipsilateral input modifies the primary somatosensory cortex response to contralateral skin flutter. J Neurosci. 2006; 26:5970–5977. [PubMed: 16738239]

Trapani G, Altomare C, Sanna E, Biggio G, Liso G. Propofol in anesthesia. Mechanism of action, structure-activity relationships, and drug delivery. Curr Med Chem. 2000; 7:249–271. [PubMed: 10637364]

Tutunculer B, Foffani G, Himes BT, Moxon KA. Structure of the excitatory receptive fields of infragranular forelimb neurons in the rate primary somatosensory cortex responding to touch. Cereb Cortex. 2006; 16:791–810. [PubMed: 16120794]

Veredas FJ, Vico FJ, Alonso JM. Factors determining the precision of the correlated firing generated by a monosynaptic connection in the cat visual pathway. J Physiol. 2005; 567.3:1057–1078. [PubMed: 16020458]

Wu CW-H, Kaas JH. Somatosensory cortex of prosimian galagos: physiological recording, cytoarchitecture, and cortiocortical connections of anterior parietal cortex and cortex of the lateral sulcus. J Comp Neurol. 2003; 457:263–292. [PubMed: 12541310]

Zeger SL, Liang K-Y. Longitudinal data analysis for discrete and continuous outcomes. Biometrics. 1986; 42:121–130. [PubMed: 3719049]

Zhu Z, Disbrow EA, Zumer JM, McGonigle DJ, Nagarajan SS. Spatiotemporal integration of tactile information in human somatosensory cortex. BMC Neurosci. 2007; 14:8–21.

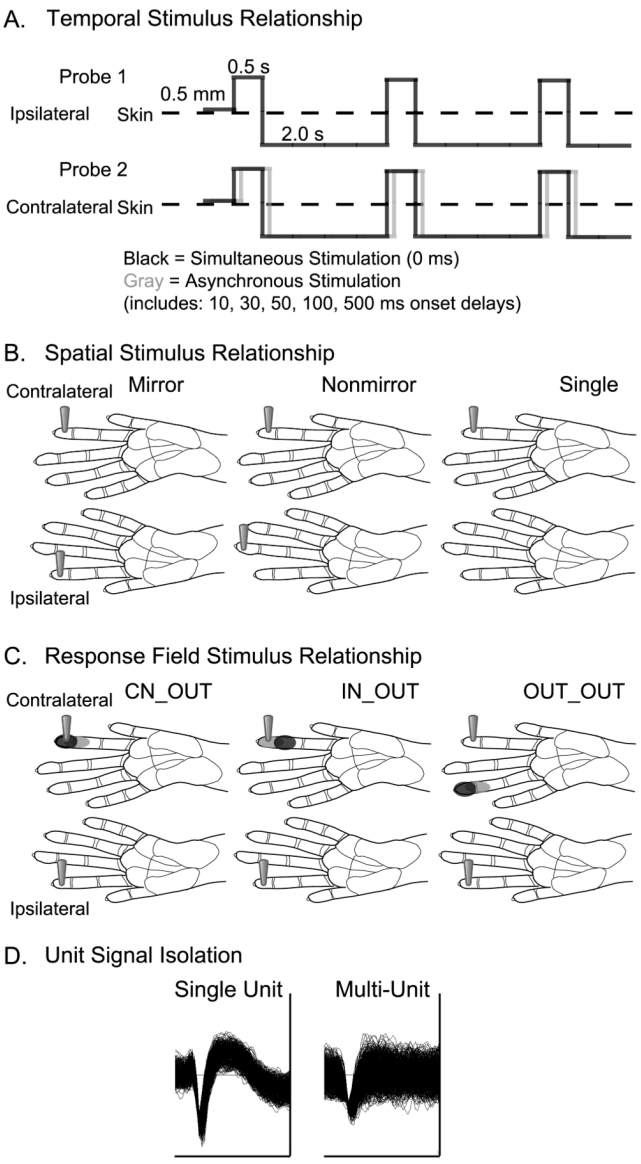

Figure 1. Schematic representations of data categories for analysis

A. The temporal pattern of stimulation is depicted by solid lines indicating the duration the stimulus probe indents the skin (0.5 s), the depth of indentation (0.5 mm), and the duration the stimulus probe is off of the skin per stimulus cycle (2.0 s). Paired stimulation, indicated by the schematics of Probe 1 and Probe 2, was simultaneous or asynchronous. To depict asynchronous stimulation generally, the gray solid line representing Probe 2 is shifted relative to the black solid line. The two probes are presented to different skin sites on the hand; however, the schematic depicts the overlap in contact time of the stimuli presented via Probe 1 and Probe 2. **B.** The spatial stimulus relationships were divided into 3 categories, illustrated by the locations of the stimulus probes on schematics of the owl monkey hands for dual probes on two hands (mirror and non-mirror locations) and a single probe on one hand as a control category. **C.** The Response Field category is determined by the unit's Response Field relative to the stimulation location. Black shading on schematics of the owl monkey hand indicates the center of the Response Field for a hypothetical unit. Gray shading on the hand indicates locations inside the Response Field, but outside the center

"hotspot" for the hypothetical reference unit. The locations of the two probes indicate the location of the stimulation relative to the Response Field for each Response Field category. **D.** Data were also classified by the quality of the signal isolation into single units or multi-units. Examples of each unit type are shown from monkey case B. The trace window for each unit shown span 128 μV and 1.6ms.

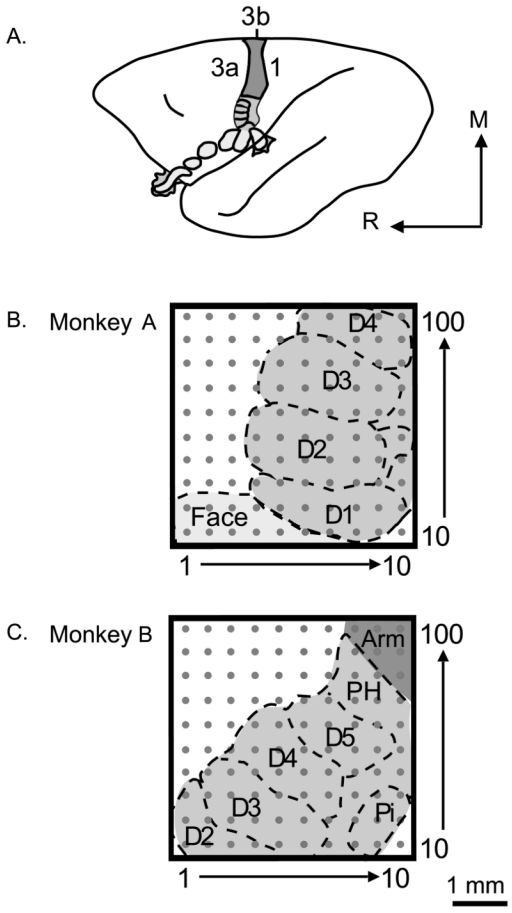

Figure 2. Schematic reconstructions show 100-electrode array placement in S1 of two owl monkey cases

A. A schematic of the owl monkey brain is shown with area 3b highlighted, as neurons in areas 3a and 1 tend not to respond well to light tactile stimulation under the anesthetic conditions of these experiments. The orientation of the brain is indicated by the arrows, with R = rostral and M = medial. **B–C.** Electrode locations in each owl monkey case were approximated based on examination of myelin-stained sections of flattened cortex and the results of receptive field mapping during recording experiments to estimate the digit and palm pad representations. The placements of the 100-electrode array in each case tended to cover a large part of the area 3b hand representation. The 1mm scale bar refers to the array size for both monkey cases.

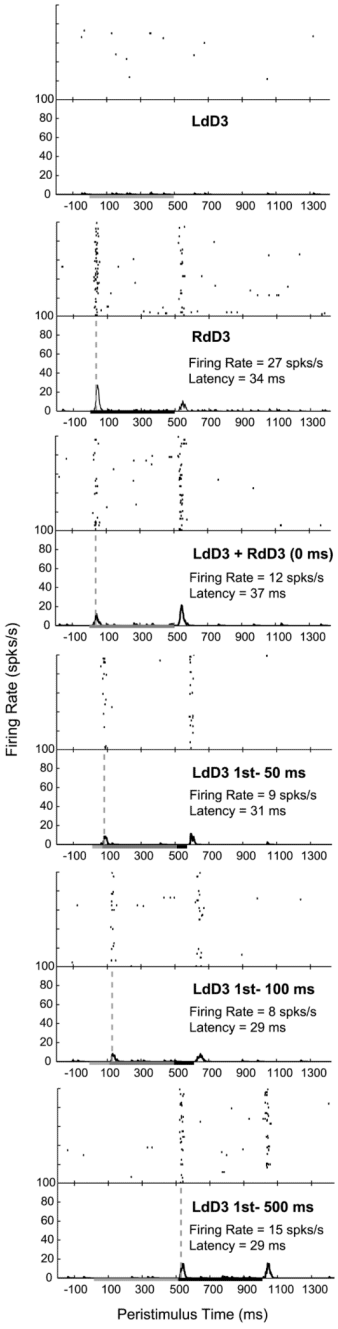

Figure 3. Example histograms from a single unit depict peak firing rate and latency changes in response to bimanual stimulation on mirror locations

The traces of the unit waveforms recorded for the given stimulation series are inset in the upper left histogram (unit 074a from case A). Histograms are shown for the neuron's responses when the locations on each hand were stimulated individually, then for both locations simultaneously, and finally for stimulus blocks in which the ipsilateral (left hand) stimulus was presented at intervals before the onset of the contralateral (right hand) stimulus. (Six out of eight stimulation conditions recorded are shown.) Stimulation was presented in blocks of 100 trials. Histograms were smoothed by a spike density function. Vertical dashed lines indicate when the latency was determined in Matlab using the criteria

described in the Methods. The duration for each stimulus was 500ms, as indicated by the line on the x-axis; therefore, paired stimulation overlapped in time for all stimulus onset delays tested except for 500ms. The measures we examined in the present study were only the peak firing rate within 50ms of the contralateral stimulus onset and the associated latency of that response. The peak firing rates were suppressed by bimanual stimulation in this example. Contralateral stimulation alone resulted in a peak firing rate (with baseline activity subtracted) of 27 spikes/s, while the firing rate response dropped to its lowest level of 8 spikes/s when the ipsilateral stimulus preceded the contralateral stimulus by 100ms.

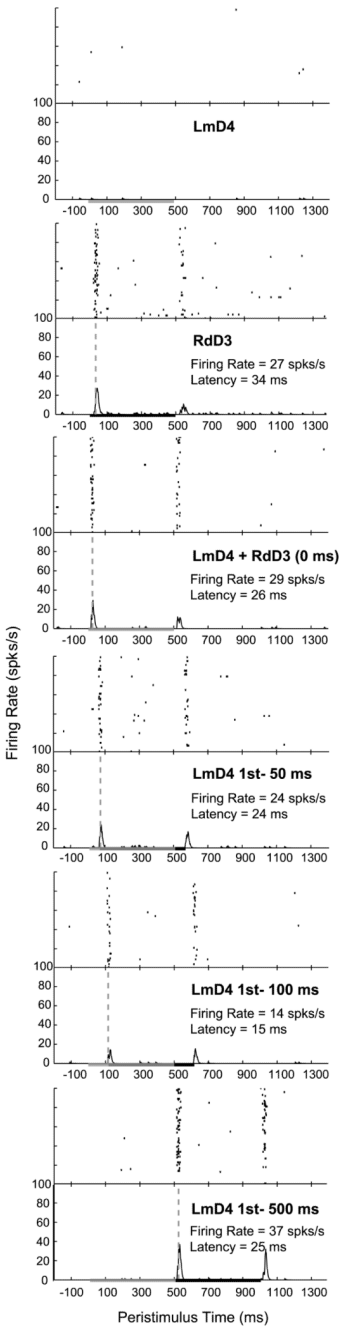

Figure 4. Example histograms from a single unit depict peak firing rate and latency changes in response to bimanual stimulation on non-mirror locations

The traces of the unit waveforms recorded for the given stimulation series are inset in the upper left histogram (unit 074a from case A, same as Figure 3). Stimulation on non-mirror locations resulted in less suppression in the same unit shown in Figure 3 compared to responses during stimulation on mirror locations. In both cases, the firing rate response dropped to its lowest level (14 spikes/s) when the ipsilateral stimulus preceded the contralateral stimulus by 100ms.

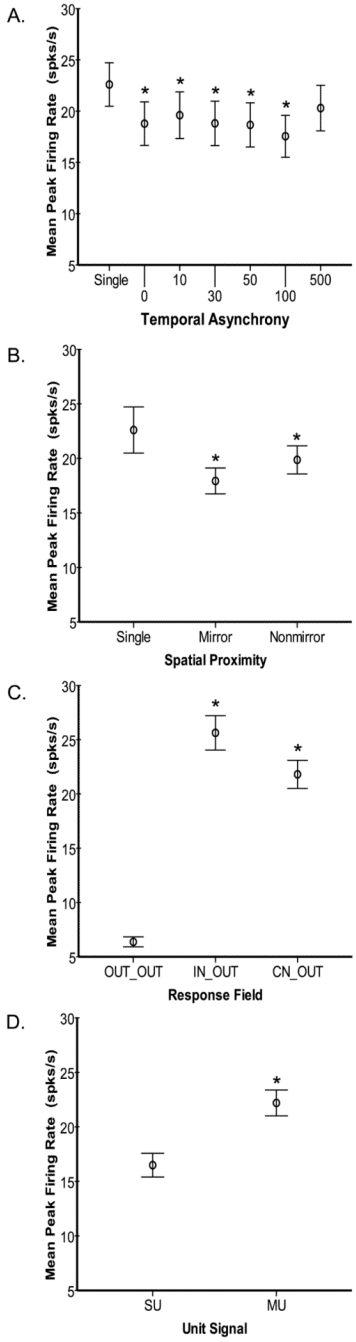

Figure 5. Average response magnitudes differ across spatial and temporal stimulus factors

Plots of group averages shown for spatiotemporal stimulus categories. Error bars represent 95% confidence intervals for all panels. **A.** Means of peak firing rate values (spikes/s) are plotted for each temporal stimulation category. Control stimulation on the contralateral location resulted in significant differences from all of the other groups except for the 500ms stimulus onset delay group. The 100ms delay group was significantly different from all other groups. The 500ms delay group was significantly different from all other groups except for 10ms (and the contralateral control group). All other comparisons not noted were significantly different. **B.** Means of peak firing rate values are plotted for the two spatial proximity categories: “Mirror” and “Non-mirror”. These two groups were not significantly

different. **C.** Means of peak firing rate values are plotted for each type of relationship of the Response Field to the stimulus locations. Peak firing rates were lower when the stimuli were outside of the Response Field (OUT_OUT) compared to when the contralateral stimulus was inside the RF (IN_OUT and CN_OUT), and the IN_OUT and CN_OUT groups were not significantly different from each other. **D.** Means of peak firing rate values are plotted for single units and multi-units, averaged across all stimulus conditions. Multi-units (MU) tended to have higher peak firing rates than single units (SU).

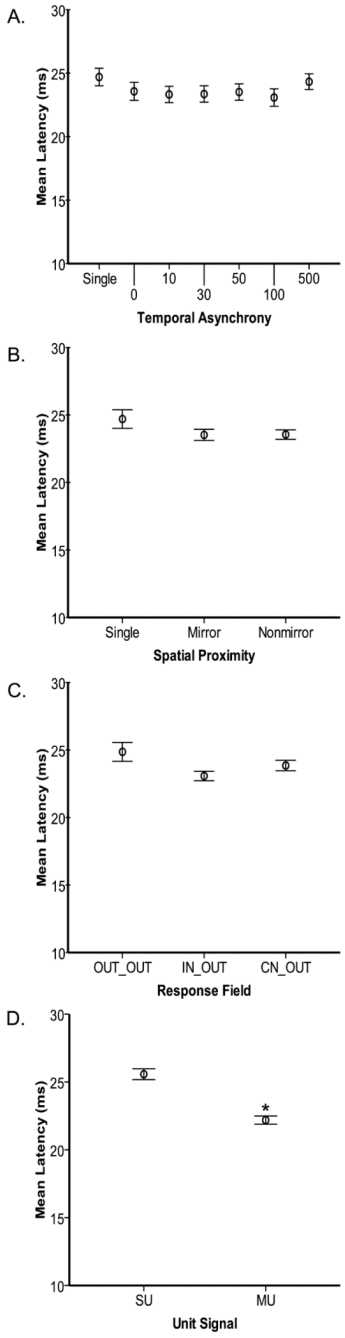

Figure 6. Average response latencies show few differences across spatial and temporal stimulus factors

Conventions follow Figure 5. Error bars represent 95% confidence intervals for all panels. **A.** Mean response latencies (ms) are plotted for each temporal stimulation condition. The control refers to the contralateral stimulus, and numbers refer to the delay between the onset of the ipsilateral stimulus and the onset of the contralateral stimulus (second) from 0 to 500ms. No pairwise comparisons were significantly different. **B.** Mean response latencies are plotted for conditions in which the stimulation locations on the two hands were in matched locations on mirror digits (Mirror) and when the stimulation sites were located on different digits of the two hands (Non-mirror). The mean latencies were not significantly

different. **C.** Mean response latencies are plotted for the relationships of the Response Field of the neurons to the stimulus locations. Latencies were longer when both stimuli were presented outside of the neuron's Response Field (OUT_OUT) compared to when the contralateral stimulus was inside the Response Field (IN_OUT and CN_OUT). **D.** Mean response latencies are plotted for single units and multi-units, averaged across all stimulus conditions. Multi-units (MU) tended to have shorter latencies than single units (SU).

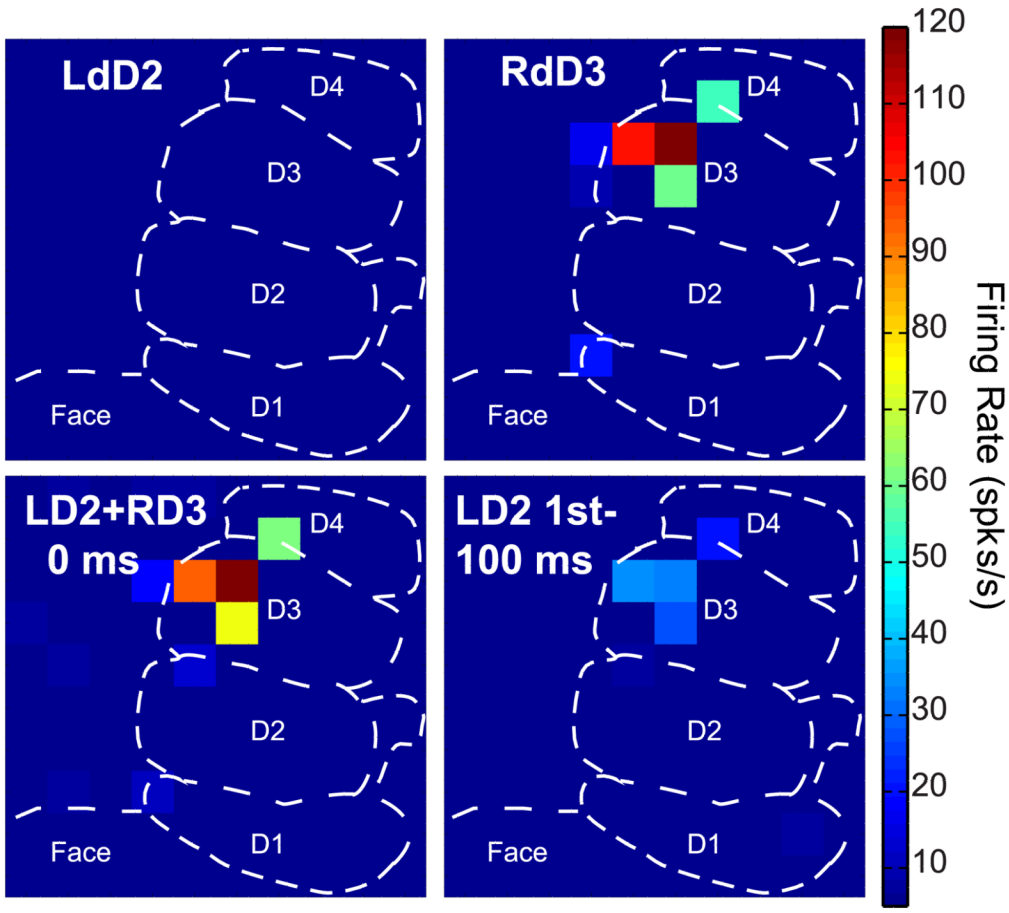

Figure 7. Peak firing rates represented as color maps across the 100-electrode array during bimanual stimulation

Examples of the peak firing activity across the multi-electrode array are shown under four experimental conditions in monkey A. Each square represents an electrode in the array and the peak firing rate value of the unit with the highest firing rate averaged over 100 trials during the 50ms response window. The color scale ranges from 5 to 120 spikes/s, with hot colors representing higher peak firing rates. Electrodes from which no significant responses were obtained during the stimulation are indicated in dark blue (no squares). The dashed lines indicate approximate locations of the representations within area 3b. **A.** Peak firing rates in case A during a stimulation series on mirror locations on distal digit 2 (dD2) show that no driven activity (> 5 spikes/s) was found when a single site on the ipsilateral digit was stimulated (top left). As expected, activity was evoked when the contralateral distal digit 3 (dD3) was stimulated (top right). When the two non-mirror sites were stimulated simultaneously (lower left), peak firing rates decreased on average across the recording area; however, the effect was not uniform. When the ipsilateral digit was stimulated 100ms before the onset of the contralateral stimulus, the firing rates were suppressed (lower right). This is one example of the response patterns that were summarized by quantifying the modulation of individual neurons across conditions.

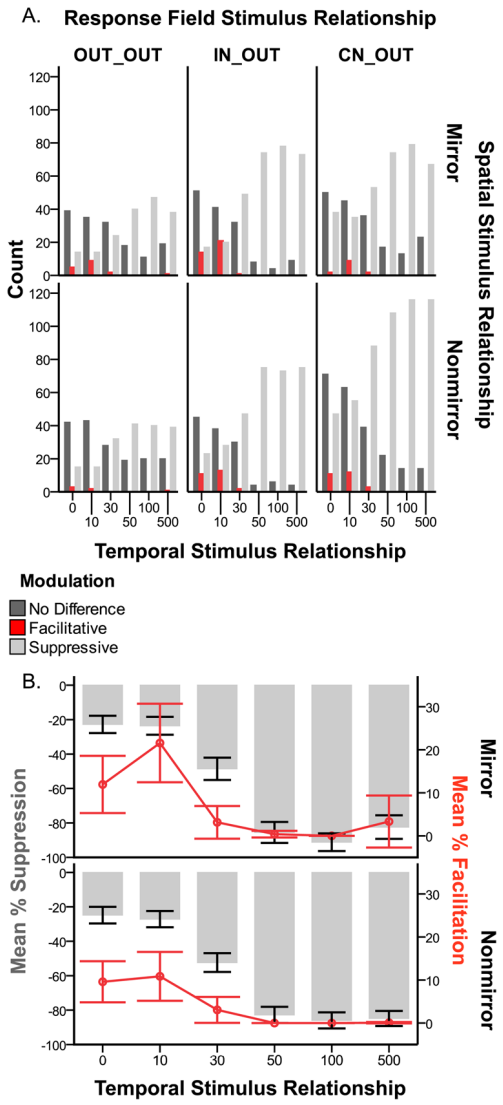

Figure 8. Suppression dominates firing rate modulation across spatiotemporal stimulus conditions

A. Comparing the expected sum of the responses to ipsilateral and contralateral stimulation to the actual responses resulted in modulation categories of: “No Difference” compared to the response to the contralateral stimulus alone, “Facilitative” compared to the summation of the responses of the controls, and “Suppressive” compared to the response to the contralateral control. Shaded bars represent the modulation categories. The types of paired stimulation conditions are grouped on the x-axis referring to the stimulus onset delays from 0 to 500ms, in which the contralateral stimulus was always presented after the ipsilateral stimulus. The row panels show the total counts of these categories for the two spatial stimulus proximity categories, “Mirror” and “Non-mirror”. The column panels divide the data based on the Response Field category: “OUT_OUT”, “IN_OUT”, and “CN_OUT”. As expected, we collected fewer responses to stimulation when both stimulation sites were outside the Response Field of the neuron, and the counts reflect this, but the trends were the same across the categories. Suppression dominated the modulation types, particularly at longer stimulus onset delays (50–500ms); whereas many responses were classified as “no difference” for short stimulus onset delays (0–30ms). Facilitation occurred rarely, but was

predominantly found when the stimulus onset delays were short (0–30ms). **B.** The percentage of facilitation and suppression was quantified to provide an index for how much the peak firing rates during paired stimulation differed from expected across the temporal stimulation conditions (x-axis). The values are collapsed across the Response Field categories, but separate panels show the effects for stimulation on Mirror locations and Non-mirror locations. The plots have dual y-axes such that the mean percentage of suppression in each category is shown by the gray bars and the values follow the left axis. The mean percentage of facilitation is shown by the red line and data markers and the values follow the right axis. Error bars are 95% confidence intervals. Using this index, when the response to paired stimulation does not differ from the contralateral response, the value is zero. The average percentages for suppression and facilitation include the zero values. The magnitude of facilitation dropped near zero when stimulus onsets were separated by 50–500ms and hovered around a 10% difference when stimulus onsets were closer in time. The average magnitude of suppression was low when the stimulus onsets were close in time, and increased when the stimulus onsets were separated by longer delays. Responses were suppressed the most on average, by 92%, when mirror locations were stimulated with a 100ms delay in stimulus onsets.

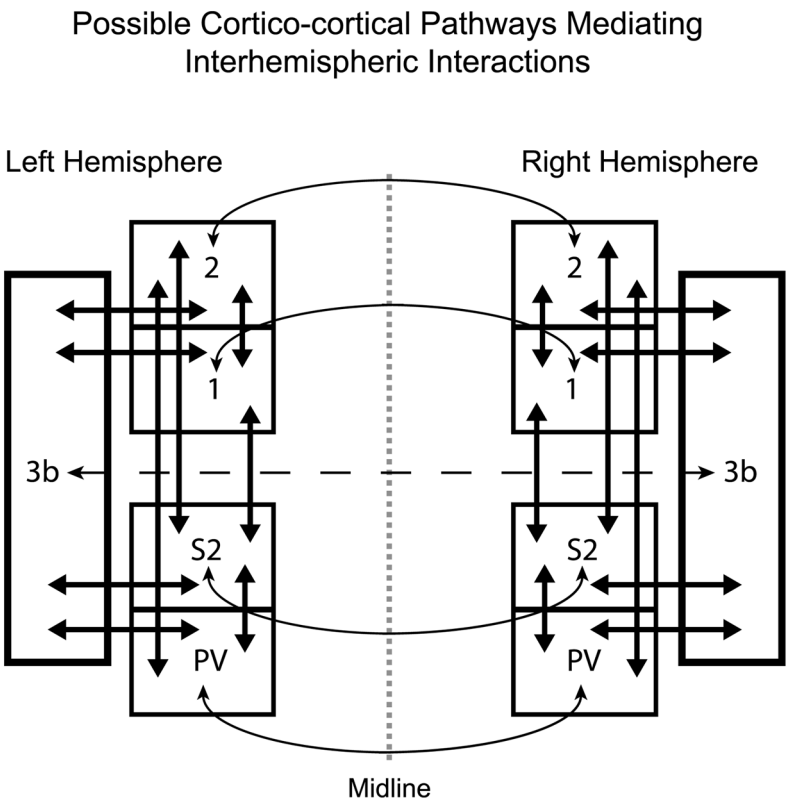

Figure 9. Inter- and intrahemispheric connections in monkeys possibly mediating interhemispheric interactions in area 3b

Schematic diagram of selected somatosensory cortical areas that may mediate interhemispheric interactions in area 3b. Connections indicated are based on neuroanatomical studies and reviews (Killackey et al., 1983; Krubitzer and Kaas, 1990; Kaas, 2000; Wu and Kaas, 2003). The dotted vertical line indicates the midline separating the two cerebral hemispheres. Intrahemispheric connections are shown with thick arrows and interhemispheric connections are shown with thin arrows. The interhemispheric connection between the hand representations of area 3b is sparse (Killackey et al., 1983) and is shown by a dashed line. Otherwise, the schematic is not drawn to represent the scale of areas or the density of connections. However, the schematic illustrates the known pathways through which neurons in area 3b may be influenced by the opposite hemisphere. Note that there are no known direct ipsilateral pathways for information from the hand, thus, subcortical somatosensory areas are not shown.

Table 1

Summary of stimulation locations and conditions

Condition	Paired Location	Monkey
Mirror	LdD2+RdD2	2
	LdD3+RdD3	2
	LdD4+RdD4	3
	LP3+RP3	3
Nonmirror	LmD3+RdD2	2
	LmD4+RdD2	2
	LdD2+RdD3	2
	LmD4+RdD3	2
	LdD4+RdD3	2
	LdD5+RdD4	3
	LdD5+RP3	3

Abbreviations: L = left; R = Right; D = digit; P = Palm pad; d = distal; m = middle

Table 2

Tests of model effects for variance in peak firing rate classified by spatial and temporal stimulus characteristics, unit type, and interactions

Variance Source	Wald Chi-Square	df	P value
(Intercept)	3542.320	1	< 0.0005
Temporal Relationship	41.450	5	< 0.0005
Spatial Relationship	0.140	1	0.709
Response Field (RF)	173.406	2	< 0.0005
Unit Type	4.354	1	0.037
Temporal x Spatial	21.475	5	0.001
Temporal x RF	41.138	12	< 0.0005
Temporal x Unit	5.259	6	0.511
Temporal x Spatial x RF	12.228	12	0.428
Temporal x Spatial x RF x Unit	41.858	32	0.114

Tests of model effects using Type III analysis from Generalized Linear Modeling with General Estimating Equations on the dependent variable peak firing rate. N = 522 units with correlated measures from the 7 levels of the variable “Temporal Relationship” (observations = 3654).

Table 3

Tests of model effects for variance in latency classified by spatial and temporal stimulus characteristics, unit type, and interactions

Variance Source	Wald Chi-Square	df	P value
(Intercept)	86865.269	1	< 0.0005
Temporal Relationship	9.401	5	0.094
Spatial Relationship	0.000	1	0.983
Response Field (RF)	5.089	2	0.079
Unit Type	35.201	1	< 0.0005
Temporal x Spatial	18.025	5	0.003
Temporal x RF	11.380	12	0.497
Temporal x Unit	2.548	6	0.863
Temporal x Spatial x RF	18.678	12	0.097
Temporal x Spatial x RF x Unit	28.147	32	0.662

Tests of model effects using Type III analysis from Generalized Linear Modeling with General Estimating Equations on the dependent variable latency. N = 522 unit subjects with correlated measures from the 7 levels of the variable “Temporal Relationship” (included observations = 2875, missing observations = 779).